

Kernel-based Adaptive Image Sampling

Jianxiong Liu, Christos Bouganis and Peter Y. K. Cheung

Department of Electrical and Electronic Engineering, Imperial College London, London, U.K.

Keywords: Progressive, Image Sampling, Kernel Regression.

Abstract: This paper presents an adaptive progressive image acquisition algorithm based on the concept of kernel construction. The algorithm takes the conventional route of blind progressive sampling to sample and reconstruct the ground truth image in an iterative manner. During each iteration, an equivalent kernel is built for each unsampled pixel to capture the spatial structure of its local neighborhood. The kernel is normalized by the estimated sample strength in the local area and used as the projection of the influence of this unsampled pixel to the consequent sampling procedure. The sampling priority of a candidate unsampled pixel is the sum of such projections from other unsampled pixels in the local area. Pixel locations with the highest priority are sampled in the next iteration. The algorithm does not require to pre-process or compress the ground truth image and therefore can be used in various situations where such procedure is not possible. The experiments show that the proposed algorithm is able to capture the local structure of images to achieve a better reconstruction quality than that of the existing methods.

1 INTRODUCTION

Progressive Image Transmission (PIT) is a family of methods that aims to make efficient use of the limited bandwidth to transmit large image data (Tzou, 1986). The system can stop at any time during the transmission and still be able to reconstruct an approximation to the ground truth image. Algorithms designed for PIT are able to rearrange the order of transmission so that significant data is transmitted first. The significance is determined by the application and it is most commonly defined as the potential of bringing a high improvement to the quality of reconstructed image.

Early designs of PIT algorithm include the Bit-Plane method (BPM) which is the basic technique categorized as one of the spatial domain techniques by the author (Tzou, 1986). Chang and Shiue (Chang et al., 1999) proposed an improved method based on BPM but all BPM-based algorithms require high transmission bandwidth. Later, various other algorithms based on vector quantization were proposed, including side-match PIT scheme (Chen and Chang, 1997) and the selective PIT (Jiang et al., 1997). There are also techniques based on point sampling and triangulation. Siddavatam Rajesh proposed a progressive image sampling technique inspired by the lifting scheme of wavelet generation and the sampled pixels are used in non-uniform B-Spline to approx-

imate the ground truth image (Rajesh et al., 2007). Demaret developed a similar method by using adaptive thinning algorithm (Demaret et al., 2006) to identify the significant pixels. Verma et al. proposed to use gradient information as significance of pixels and use linear bivariate splines to reconstruct (Verma et al., 2010). There are also techniques based on transform domain. The Discrete Cosine Transform (DCT) and Discrete Wavelet Transform (DWT) were used in many techniques to transform the image to frequency domain. Such transforms are used in the popular JPEG and JPEG2000 standards (Skodras et al., 2001) (Chang et al., 2008) (Chang and Lu, 2006) as the pre-processing stage of the compression process. Based on the transformed image, further discussions about the progressive transmission of the coefficients were made. The coefficients can be transmitted progressively in a hierarchical way, or in more complicated manner such as that proposed by Shapiro (Embedded Zerotree Wavelet coder (Shapiro, 1993)) or later by Amir Said (Set Partitioning in Hierarchical Trees (Said and Pearlman, 1996)).

Despite of the many techniques developed in the past decade, few of them can operate without pre-processing the image. Most of the techniques require to analyze the ground truth image first to find out an optimized order of transmitting the data. However in practice many applications, such as graphics render-

ing and range sampling, do not have the ground truth image readily available – sampling can only be done in a blind way. In such applications, it is often expensive to sample a pixel and therefore the concept of PIT also applies well. Non-uniform stochastic point sampling is often used in these situations where the statistics of the image to sample is unknown. Eldar et al. (Eldar et al., 1997) proposed the Farthest Point Strategy (FPS) as a stochastic model that ensures maximum sample distance. He also introduced the data adaptive version of FPS (AFPS) to benefit from previously sampled pixels. Later, Devir successfully applied this idea in range sampling system and generalized it to accommodate grid sampling (Devir and Lindenbaum, 2007).

This paper proposes a progressive image sampling technique that does not require pre-processing of the ground truth image. The proposed technique samples an amount of pixels at each iteration, based on estimated pixel priority from previous samples. The pixel priority is modeled by building equivalent kernels which adapt to the local embedded structure of the image. The rest of the paper is arranged as follows: In section II we will generalize the problem of progressive point sampling; in section III we will explain the details of the proposed technique; finally experimental results are listed and discussed in Section IV, showing the improved ability of the system to identify and sample significant pixels at early stage, resulting in an improved reconstruction quality.

2 GENERALIZED FRAMEWORK OF POINT SAMPLING

In situations where the ground truth image is not readily available, stochastic point sampling is suggested to have advantages over uniform sampling (Eldar et al., 1997). An approximation to the image can be reconstructed from the non-uniformly sampled pixels by interpolation based on triangulation technique. Conventional point sampling algorithms are designed to generate sampling patterns ensuring both randomness and maximum distance. The randomness is introduced to reduce the effect of potential aliasing while the maximum distance is based on the basic assumption of signal continuity. On top of that, the sampling process can be refined iteratively to better adapt to the sampled data. As proposed by Eldar et al., the sampling process can be data adaptive by modeling the priority score of each candidate unsampled pixel to be the product of its Euclidean distance to the nearest sampled pixel and its estimated local bandwidth. To ensure the maximum distance, candidates in AFPS

are always the Voronoi vertices of the triangulation formed by the already sampled pixels. As shown in Fig.1, the candidate unsampled pixel i has a priority score determined by the three vertices of the enclosing triangle (Eldar et al., 1997):

$$f(\mathbf{x}_i) = \|\mathbf{x}_i - \mathbf{x}_{s_1}\|_2 * \max_{k \neq 1} (B_{\min}(\mathbf{x}_{s_k}, \mathbf{x}_{s_l})) \quad (1)$$

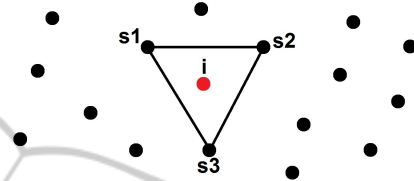


Figure 1: AFPS example: black dots are already sampled pixels.

This priority score was extended from Voronoi vertices to all unsampled pixels in (Devir and Lindenbaum, 2007) to allow sampling on regular grid:

$$f(\mathbf{x}_i) = \min_{k=1,2,3} (\|\mathbf{x}_i - \mathbf{x}_{s_k}\|_2) * \log(1 + \hat{\sigma}^2) \quad (2)$$

Where $\hat{\sigma}$ is the weighted local variance of point \mathbf{x}_i .

We further extend the concept to a more general form for point sampling as the product of distance term and variance term:

$$f(\mathbf{x}_i) = d_{\mathbf{x}_i, P} * v_i \quad P : \text{sampled pixel locations} \quad (3)$$

Where \mathbf{x}_i is the coordinate vector of a candidate unsampled pixel, and $d_{\mathbf{x}_i, P}$ measures the likelihood of determining pixel \mathbf{x}_i with existing samples. This distance therefore includes but is not limited to Euclidean distance. The term v_i is the estimated variance of pixel \mathbf{x}_i . In the next section, we will explain in detail how to model the two terms using equivalent kernels, to better capture the embedded spatial structure of natural images.

3 ADAPTIVE SAMPLING WITH EQUIVALENT KERNEL

In (Takeda et al., 2007), Takeda et al. generalized the use of kernels in image regression. Covering similar ideas such as the popular Bilateral Filter, they built a generalized framework of using the concept of kernel in regression with non-uniformly sampled pixels, as well as filtering the rough estimation to improve the image quality. In particular, they proposed to refine a rough estimation by applying the steerable

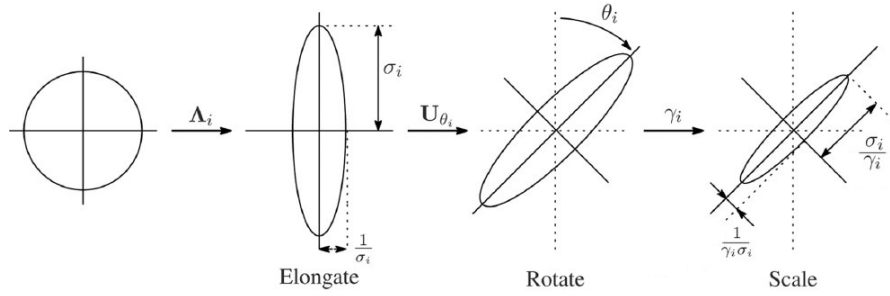


Figure 2: Effects of applying the steering matrix $\mathbf{C}_i = \gamma_i \mathbf{U}_{\theta_i} \Lambda_i \mathbf{U}_{\theta_i}^T$; the shape of the kernel is changed to reflect the local image structure (Takeda et al., 2007).

kernel, which showed the capability of kernel-based method to represent the spatial relationship between pixel pairs.

The formulation of kernel regression comes naturally from the local expansion of a universal regression function defined around sampled points. Based on the assumption of local smoothness to some order N , a relationship between a given sample and the pixel to be estimated is established. And the final estimate of the unknown pixel is formulated as a weighted sum of sampled pixels, where the weights (equivalent kernels) are determined by the geometrical and statistical correlation between a sample and the unknown pixel.

In this work however, the similar concept is used in modelling not for the regression but the sampling priority of unknown pixels at each sampling iteration. This is based on the fact that the sampling process serves the regression or interpolation process which eventually reconstructs the image. Therefore the statistical correlation between pixels derived for the kernel regression technique also applies and can guide the sampling process to prepare a more suitable sampling pattern leading to a higher reconstruction confidence.

3.1 Modeling the Variance Term

The core idea of steerable kernel, as is used in image regression, is its ability to identify the local spatial relationship between pixel locations. The construction of steerable kernel requires gradient information of the local area, which can be computed by applying Sobel operators on the rough estimate from previously sampled pixels. Although gradient information computed in this way is an approximation of the ground truth, it can still provide guidance to build steerable kernels. Without losing generality, here we make two assumptions:

1. **A1**: Assume that around each candidate unsam-

pled pixel, the samples in its neighbourhood are dense enough to provide information for the constructing of a stable steerable kernel;

2. **A2**: Assume that each unsampled pixel that is going to be interpolated after sampling steps, is of same importance to the reduction of the Mean Squared Error of the reconstructed image.

It is worth noting that **A1** is always an approximation in practice, although it serves as the foundation to the construction of kernels in related techniques. For kernel regression, **A1** directly impacts the reconstruction quality of the image. However for the purpose of point sampling as this work does, the requirement is more relaxed because the model is continuously being refined and **A1** becomes more accurate during the course.

Instead of directly modeling the variance of an unsampled pixel, we first model the relationship between the pixel in question or in other words, project its requirement of information to its neighborhood. If we set the order $N = 0$, i.e. Nadaraya-Watson Estimator (NWE), the classic kernel regression sees the kernel centered on an unsampled pixel \mathbf{x} to be:

$$\hat{K}(\mathbf{x}_i) = \frac{K_h(\mathbf{x}_i - \mathbf{x})}{\sum_{\mathbf{x}_j} K_h(\mathbf{x}_j - \mathbf{x})}, K_h(t) = \frac{1}{h} K\left(\frac{t}{h}\right), \mathbf{x}_i \in P \quad (4)$$

Where h is the global smoothing parameter and P is the collection of samples in the local area. The regression is essentially a weighted sum of the local samples and it reflects the basic continuity assumption behind image interpolation. To model for the sampling process, notice that this kernel function can also be computed on Q , the collection of unsampled pixels, to form a complete kernel in the local area. The weights on unsampled pixels, indicated by this kernel, can be regarded as their potential correlation with \mathbf{x}_i .

To take into consideration of the local spatial structure, the global smoothing parameter is modified

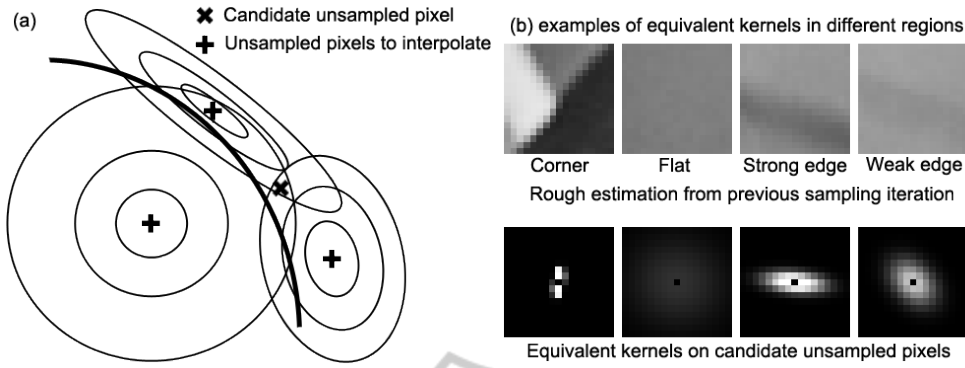


Figure 3: Examples of equivalent kernel. The kernel shows a strong correlation among pixels along estimated edges; on flat surface the kernel is more spread out, reflecting a more unbiased connection with neighboring pixels; on corner regions, the kernel is very centered due to a complex embedded structure. The accumulated kernel value on the candidate unsampled pixel in (a), projected from neighbouring samples, reflects the variance or freedom of this pixel during the reconstruction process.

to local smoothing matrix $\mathbf{H}_{\mathbf{x}}^{steer} = h * \mathbf{C}_{\mathbf{x}}^{-\frac{1}{2}}$. Where the covariance matrix $\mathbf{C}_{\mathbf{x}}$ can be computed by:

$$\mathbf{C}_{\mathbf{x}} = \gamma_{\mathbf{x}} \mathbf{U}_{\theta_{\mathbf{x}}} \Lambda_{\mathbf{x}} \mathbf{U}_{\theta_{\mathbf{x}}}^T \quad (5)$$

$$\mathbf{U}_{\theta_{\mathbf{x}}} = \begin{bmatrix} \cos \theta_{\mathbf{x}} & \sin \theta_{\mathbf{x}} \\ -\sin \theta_{\mathbf{x}} & \cos \theta_{\mathbf{x}} \end{bmatrix} \quad (6)$$

$$\Lambda_{\mathbf{x}} = \begin{bmatrix} \sigma_{\mathbf{x}} & 0 \\ 0 & \sigma_{\mathbf{x}}^{-1} \end{bmatrix} \quad (7)$$

The parameter set $(\sigma_{\mathbf{x}}, \theta_{\mathbf{x}}, \gamma_{\mathbf{x}})$ is computed from singular value decomposition of the matrix of local gradients. If $z_{x_1}(\cdot)$ and $z_{x_2}(\cdot)$ are first derivatives of the grayscale value along x_1 and x_2 directions respectively, then the decomposition of the gradient matrix in the neighborhood is:

$$\begin{bmatrix} \vdots & \vdots \\ z_{x_1}(\mathbf{x}_j) & z_{x_2}(\mathbf{x}_j) \\ \vdots & \vdots \end{bmatrix} = \mathbf{U}_{\mathbf{x}} \mathbf{S}_{\mathbf{x}} \mathbf{V}_{\mathbf{x}}^T, \quad \mathbf{x}_j \in P \cup Q \quad (8)$$

The rotation angle $\theta_{\mathbf{x}}$ is computed from $\mathbf{v}_2 = [\mathbf{v}_1, \mathbf{v}_2]$, the second column of the orthogonal matrix $\mathbf{V}_{\mathbf{x}}$.

$$\theta_{\mathbf{x}} = \arctan\left(\frac{\mathbf{v}_1}{\mathbf{v}_2}\right) \quad (9)$$

The elongation parameter is the ratio of the energy in the two dominant directions, indicated by the two diagonal elements of $\mathbf{S}_{\mathbf{x}}$: $\sigma_{\mathbf{x}} = s_1/s_2$. The scaling parameter $\gamma_{\mathbf{x}}$ is determined by the geometric mean of the energy normalized by the number of pixels M in the neighbourhood: $\gamma_{\mathbf{x}} = \sqrt{s_1 s_2}/M$. The effect of applying the steering matrix on the kernel function is shown in Fig.2.

The final equivalent kernel constructed with the steerable smoothing matrix in the local area is then defined as:

$$\hat{K}_{\mathbf{x}}(\mathbf{x}_i) = \frac{K_{\mathbf{H}_{\mathbf{x}}^{steer}}(\mathbf{x}_i - \mathbf{x})}{\sum_{\mathbf{x}_i} K_{\mathbf{H}_{\mathbf{x}}^{steer}}(\mathbf{x}_i - \mathbf{x})}, \quad \mathbf{x}_i \in P \cup Q \quad (10)$$

$$K_{\mathbf{H}_{\mathbf{x}}^{steer}}(\mathbf{x}_i - \mathbf{x}) = \frac{\sqrt{\det(\mathbf{C}_{\mathbf{x}})}}{2\pi h^2} \exp\left\{-\frac{(\mathbf{x}_i - \mathbf{x})^T \mathbf{C}_{\mathbf{x}} (\mathbf{x}_i - \mathbf{x})}{2h^2}\right\} \quad (11)$$

The equivalent kernel constructed in this way is regarded as an ‘‘ideal kernel’’ that describes the local structure of the image. It is centered on each unsampled pixel and covers a local area around it. It is computed from local statistics (A1), and is normalized to have a sum of 1 to reflect the same amount of influence each unsampled pixel is able to project to its neighborhood (A2). If $\mathbf{x}_i \in Q$, a large $\hat{K}_{\mathbf{x}}(\mathbf{x}_i)$ indicates that as a candidate unsampled pixel \mathbf{x}_i being sampled next will make \mathbf{x} more likely to be interpolated accurately due to its high correlation with \mathbf{x}_i . The variance term in (3) is therefore the sum of all the pair-wise relationship between a candidate unsampled pixel \mathbf{x}_i and other unsampled pixels in its neighborhood:

$$v(\mathbf{x}_i) = \sum_{\mathbf{x}_i \in Q} \hat{K}_{\mathbf{x}}(\mathbf{x}_i), \quad \mathbf{x}_i \in Q_{global} \quad (12)$$

An example of accumulating for the variance term is given in Fig.3. In this example, the candidate unsampled pixel in the middle has an accumulated variance score from other unsampled pixels in the neighborhood, all of which have their own equivalent kernels centered on them. The candidate can be any unsampled pixel, or certain pixel locations selected by other algorithms, such as those that happen to be Voronoi vertices at the same time.

Given all the unsampled pixels $\mathbf{x} \in Q$ to interpolate, a higher variance term $v(\mathbf{x}_i)$ indicates that sampling \mathbf{x}_i is likely to reduce a large amount of collective variance of its neighborhood, therefore is more capable of stabilizing the local interpolation and has a bigger impact to improving the image quality.

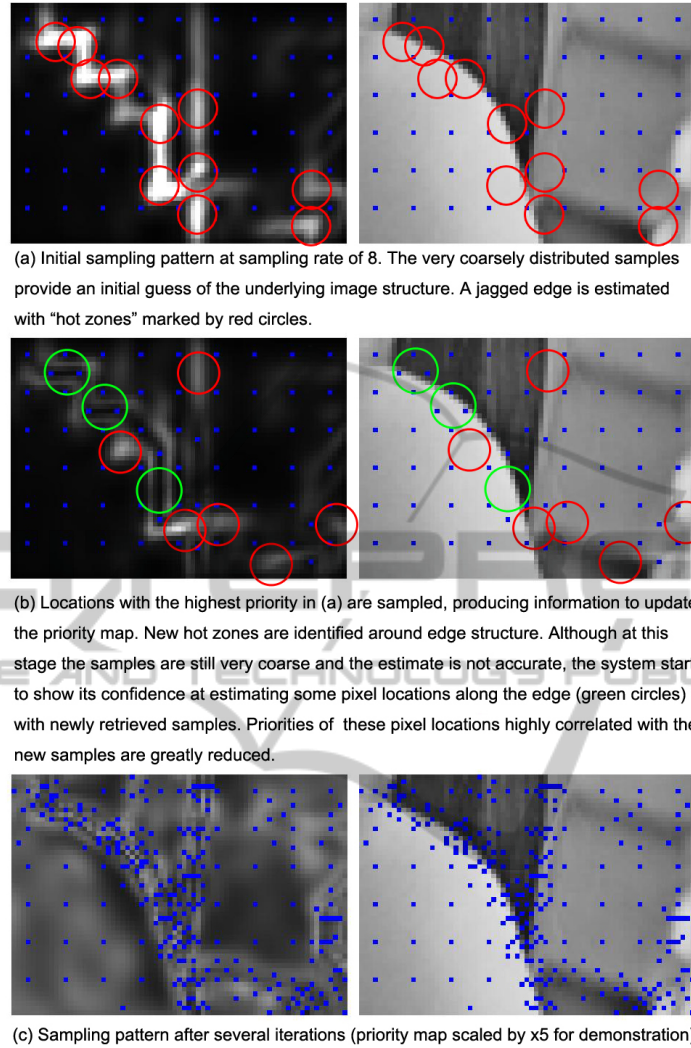


Figure 4: Example of the sample process. Blue dots are sampled locations; graphs on the left hand side are priority maps in grayscale, showing candidate pixel locations with higher priority score $f(\mathbf{x}_i)$ in brighter dots; pictures on the right hand side are the original image patch.

3.2 Modeling the Distance Term

Although unsampled, some pixels are more determined than others because within its neighborhood, more highly correlated pixels have already been sampled. The distance term is therefore to compensate for this effect. To measure the likelihood of determining pixel \mathbf{x} with already sampled pixels, we define the sample strength within its neighborhood to be:

$$l_P(\mathbf{x}) = \frac{\sum_{\mathbf{x}_i \in P} \hat{K}_{\mathbf{x}}(\mathbf{x}_i)}{\max_{\mathbf{x}_i \in P} (\hat{K}_{\mathbf{x}}(\mathbf{x}_i))} \quad (13)$$

It is closely related to the sample density discussed in (Takeda et al., 2007), but is normalized by the highest value of the equivalent kernel, to reflect that the

most related pixels within the neighborhood (often the closest ones) should have the maximum correlation value of 1. This is also based on the basic continuity assumption of natural images. By virtue of equivalent kernel, the sample strength takes into account both the spatial distance and the embedded image structure. A higher sample strength will reduce the total influence that an unsampled pixel is able to project to its neighborhood. The distance term of \mathbf{x} is therefore defined as:

$$d_{\mathbf{x},P} = \log(1 + 1/l_P(\mathbf{x})) \quad (14)$$

The equivalent kernel (10) of each unsampled pixel is then multiplied by their corresponding distance term according to (3). The final priority score

of a candidate unsampled pixel \mathbf{x}_i is then:

$$f(\mathbf{x}_i) = \sum_{\mathbf{x} \in Q} \hat{K}_{\mathbf{x}}(\mathbf{x}_i) \cdot d_{\mathbf{x},P}, \quad \mathbf{x}_i \in Q_{global} \quad (15)$$

3.3 The Complete Kernel-based Adaptive Sampling Algorithm

With the priority score computed from existing samples and reconstruction, at each sampling iteration a number of new samples can be taken by choosing the candidates of highest priority scores. After taking new samples, the image can be reconstructed from the non-uniformly sampled pixels using different methods. In this paper we use the Delaunay Triangulation based linear bivariate splines for demonstration purpose.

Fig.4 shows an example of the sampling process and the computed priority map of $f(\mathbf{x}_i)$. This example starts at a relatively low sampling rate which results in a coarse sampling pattern (sampled pixels are marked as blue dots). Note that the purpose of progressive image sampling is to identify and sample the most significant information of images as early as possible. In other words, it is to achieve a better approximation quality at the receiver side using as few samples as possible. Therefore the performance of such algorithms is determined by their ability to use limited/distorted information to estimated the underlying ground truth model of the target image. In reality, **A1** is always an approximation to enable such point sampling process. It is indeed the case in this particular example: the system has to use the very coarse sampling pattern to estimate the ground truth model.

The complete procedure of the design is shown in algorithm.1.

4 EXPERIMENTAL RESULTS

The proposed Kernel-based Adaptive Sampling (KbAS) was tested on multiple benchmark images and compared with the grid AFPS method (Devir and Lindenbaum, 2007). The target images to sample from are all of size 257×257 , to allow an initialized sampling pattern at the rate of 8 (take a sample every 8 pixels in each dimension) to start from. The images are grayscale and each pixel is described by 8 bits. In the test, the size of the local analysis window is set to be 17×17 and the Sobel operator is applied to a smaller local area of size 5×5 . The global smoothing parameter h is set to be an empirical value of 3. Although there are more complicated interpolation/regression methods, linear bivariate splines was

Algorithm 1: The proposed kernel-based adaptive sampling.

Require: Initial sampling pattern P_{global} and Q_{global} ; initial reconstruction of the image \hat{I} ; the maximum number of samples to take n ; number of samples to take at each step m

Ensure: The updated sampling pattern P_{global} and Q_{global} ; the updated reconstruction of the image \hat{I}

- 1: **while** (the number of pixels in P_{global}) $< n$ **do**
 - 2: Initialize a priority map L of the same size as the image to record the priority score for each pixel in Q_{global}
 - 3: Apply Sobel operators on the current reconstruction \hat{I}
 - 4: For each pixel in Q_{global} , construct an equivalent kernel using (10) and (14); then accumulate the equivalent kernel to L
 - 5: Apply a local maximum filter to L and then find out m candidates that are of the highest priority score
 - 6: Sample these m pixels from the original image and update P_{global} and Q_{global} accordingly
 - 7: Interpolate and reconstruct \hat{I} with the samples
 - 8: **end while**
 - 9: **return** updated P_{global} , Q_{global} , and \hat{I}
-

chosen in this test for its simplicity. Discussions of different reconstruction methods are beyond the scope of this article.

Fig.5 shows an example of sampling patterns generated for the image “lena”, and corresponding priority maps computed. Fig.5 (a) is the initial sampling pattern and priority map showing a rough estimate of the embedded structure. After several iterations when the number of samples reaches 4096, the resulted sampling pattern is shown in (b). Note that the priority map in (b) is scaled by x5 for a better demonstration. It can be seen from (b) that most samples are centered around complicated structures like edges or textures. However, when samples are taken the priority scores in their neighborhood decrease. Therefore the relative priorities of pixel locations that were considered insignificant increase, making them more possible to be sampled in the next iteration.

Two example reconstructions resulted from sampled pixels are given in Fig.6. It can be seen that because of the embedded prior knowledge about natural images, the proposed method provides better sampling patterns at early stage, that result in more accurate approximations of the ground truth image. Although the reconstruction algorithm is the same for

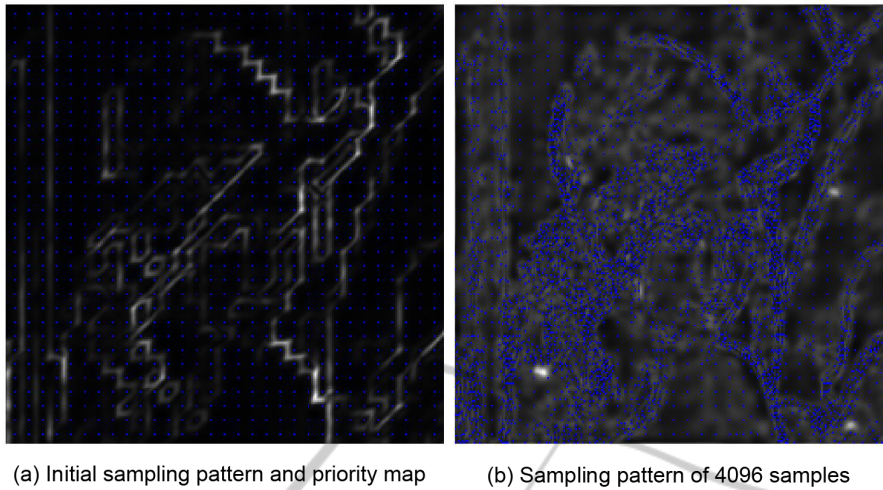


Figure 5: Example of sampling patterns of lena, and the corresponding priority maps. Blue dots are sampled pixel locations and brighter spots correspond to higher priorities.

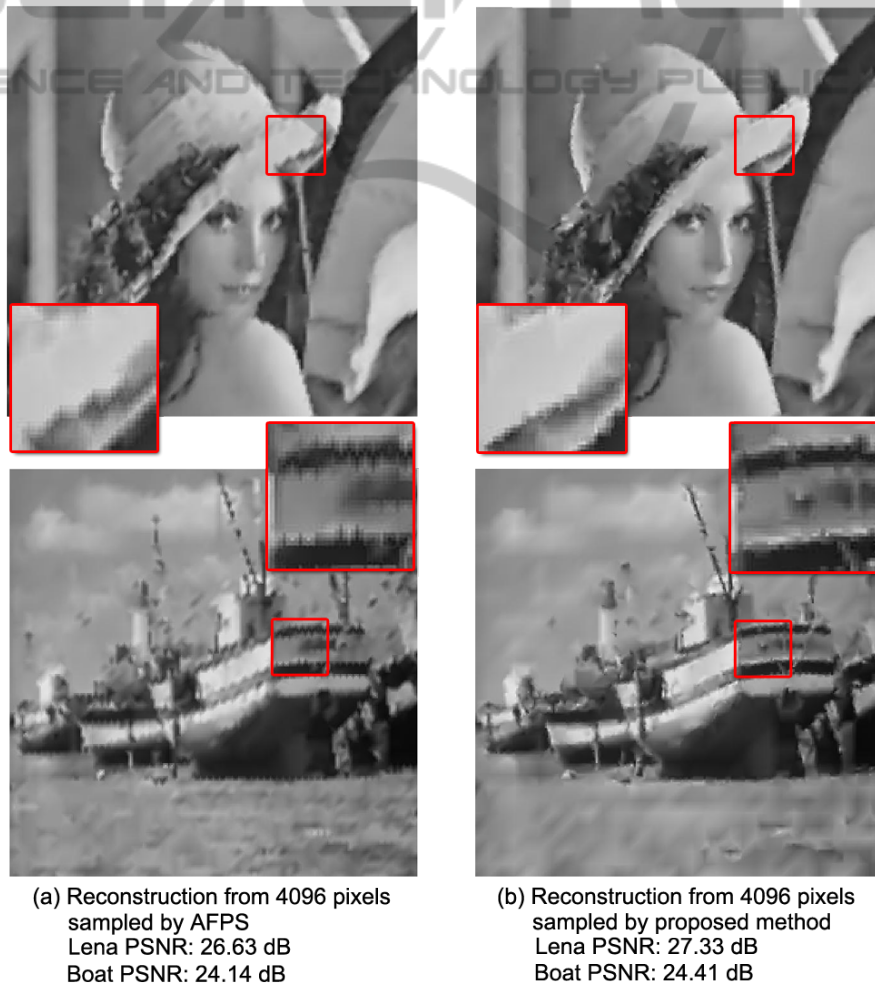


Figure 6: Result comparison with AFPS (Devir and Lindenbaum, 2007), at 4096 samples.

both sampling methods, the proposed method enhances the visual quality of the reconstructed image by focusing on sampling in structured regions such as edges. Therefore, the consequent image reconstructed from the basic linear bivariate splines has a similar sharpening effect as images enhanced by kernel regression (Takeda et al., 2007).

More experimental results are provided in Table 1, showing the ability of the proposed method to capture the embedded image structure at early stage of sampling.

Table 1: Performance comparison in PSNR (dB).

| Target | Method | 0.2 b/p | 0.3 b/p | 0.5 b/p |
|-----------|--------|---------|---------|---------|
| Lena | AFPS | 23.63 | 24.83 | 26.63 |
| | KbAS | 23.72 | 25.32 | 27.33 |
| Barbara | AFPS | 22.36 | 23.69 | 25.09 |
| | KbAS | 22.44 | 23.98 | 25.37 |
| Boat | AFPS | 21.62 | 22.62 | 24.14 |
| | KbAS | 21.95 | 22.91 | 24.41 |
| Cameraman | AFPS | 21.62 | 23.21 | 25.46 |
| | KbAS | 21.98 | 23.59 | 25.75 |
| Peppers | AFPS | 22.16 | 23.41 | 25.54 |
| | KbAS | 22.58 | 24.17 | 25.98 |

5 CONCLUSIONS

In this paper, we proposed the Kernel-based Adaptive Sampling method that is able to progressively sample/reconstruct an image, without the need of pre-processing or compression of the image. The proposed method makes use of the prior knowledge about natural images embedded in the framework of kernel construction, and is able to identify at early stages pixel locations that are more significant to improve the reconstruction quality of the image. Reconstructed images from samples retrieved from the proposed method have higher image quality measured in PSNR, as well as better visual quality by virtue of the steerable kernel modeling.

REFERENCES

- Chang, C.-C., Li, Y.-C., and Lin, C.-H. (2008). A novel method for progressive image transmission using blocked wavelets. *AEU-International Journal of Electronics and Communications*, 62(2):159–162.
- Chang, C.-C. and Lu, T.-C. (2006). A wavelet-based progressive digital image transmission scheme. In *Innovative Computing, Information and Control, 2006. ICICIC'06. First International Conference on*, volume 2, pages 681–684. IEEE.
- Chang, C.-C., Shiue, F.-C., and Chen, T.-S. (1999). A new scheme of progressive image transmission based on bit-plane method. In *Communications, 1999. APCC/OECC'99. Fifth Asia-Pacific Conference on... and Fourth Optoelectronics and Communications Conference*, volume 2, pages 892–895. IEEE.
- Chen, T. and Chang, C. (1997). Progressive image transmission using side match method. *Information Systems and Technologies for Network Society*, pages 191–198.
- Demaret, L., Dyn, N., and Iske, A. (2006). Image compression by linear splines over adaptive triangulations. *Signal Processing*, 86(7):1604–1616.
- Devir, Z. and Lindenbaum, M. (2007). Adaptive range sampling using a stochastic model. *Journal of computing and information science in engineering*, 7(1):20–25.
- Eldar, Y., Lindenbaum, M., Porat, M., and Zeevi, Y. (1997). The farthest point strategy for progressive image sampling. *Image Processing, IEEE Transactions on*, 6(9):1305–1315.
- Jiang, J., Chang, C., and Chen, T. (1997). Selective progressive image transmission using diagonal sampling technique. In *Proceedings of International Symposium on Digital Media Information Base*, pages 59–67.
- Rajesh, S., Sandeep, K., and Mittal, R. (2007). A fast progressive image sampling using lifting scheme and non-uniform b-splines. In *Industrial Electronics, 2007. ISIE 2007. IEEE International Symposium on*, pages 1645–1650. IEEE.
- Said, A. and Pearlman, W. A. (1996). A new, fast, and efficient image codec based on set partitioning in hierarchical trees. *Circuits and systems for video technology, IEEE Transactions on*, 6(3):243–250.
- Shapiro, J. M. (1993). Embedded image coding using zerotrees of wavelet coefficients. *Signal Processing, IEEE Transactions on*, 41(12):3445–3462.
- Skodras, A., Christopoulos, C., and Ebrahimi, T. (2001). The jpeg 2000 still image compression standard. *Signal Processing Magazine, IEEE*, 18(5):36–58.
- Takeda, H., Farsiu, S., and Milanfar, P. (2007). Kernel regression for image processing and reconstruction. *Image Processing, IEEE Transactions on*, 16(2):349–366.
- Tzou, K.-H. (1986). Progressive image transmission: a review and comparison of techniques. *Optical Engineering*, 26(7):267581–267581.
- Verma, R., Verma, R., Sree, P. S. J., Kumar, P., Siddavatam, R., and Ghrra, S. (2010). A fast progressive image transmission algorithm using linear bivariate splines. In *Contemporary Computing*, pages 568–578. Springer.